



Classification of Fundus Images Based on Severity Utilizing SURF Features from the Enhanced Green and Value Planes

Minal Hardas, Sumit Mathur and Anand Bhaskar

EasyChair preprints are intended for rapid dissemination of research results and are integrated with the rest of EasyChair.

June 10, 2022

Classification of fundus images based on severity utilizing SURF features from the enhanced green and value planes

Minal Hardas¹[0000-0002-9921-9576] Sumit Mathur²[0000-0002-5554-5521]
and Anand Bhaskar³[0000-0002-6255-328x]

¹Sir Padampat Singhania University, Udaipur 313601, India

^{2,3}Sir Padampat Singhania University, Udaipur 313601, India
minal.sudarshan@spsu.ac.in

Abstract. Diabetic retinopathy (DR) is a complication of longstanding diabetes that affects vision. In DR, the small blood vessels that supply the nutrients and oxygen to the retina get damaged, which can blur the vision. If not treated in the preliminary stages, DR can even lead to a complete loss of vision. Hence, a concise technique for detecting and grading the severity level of DR is necessary. The current paper focuses on an automated DR detection and severity classification technique on retinal fundus images using the Support Vector Machine (SVM) classifier. Our proposed system comprised pre-processing of the fundus images and merging the enhanced green and value color planes. The Average Grey Value Extraction (AGVE) algorithm was applied to the merged image to extract the important information from the eye. Then, the Speeded-Up Robust Features (SURF) was used to extract the strongest feature points in the fundus image. SVM was trained to classify the DR fundus images into various levels of severity. The experimentation results on the DIARETDB1 dataset obtained an average accuracy of 98.68% and an average F1 score of 0.99. A novel red score was found out to be a good indicator of severity. By combining the enhanced green and value color plane, the features extracted by SURF were more accurate for predicting the severity. Thus, the proposed system will assist the doctors in detecting the severity level of DR efficiently and reliably, enabling them to start medication on time.

Keywords: Diabetic Retinopathy, Support Vector Machine, Severity

1 Introduction

DR is a complication of diabetes that affects the eyes. It is caused by high blood sugar because of diabetes, which damages the retina [1]. The retina is provided with a supply of blood vessels and nerves. These blood vessels to the retina develop tiny swellings called microaneurysms, which are prone to hemorrhage [2]. The interruption to the supply of nutrients and oxygen triggers the formation of new blood vessels across the eye [3]. The new blood vessels formed are brittle and prone to breakage. Both the microaneurysms and the newly formed blood vessels may rupture the path. This causes the leakage of blood into the retina and blurriness of vision. DR may even lead to blindness [4]. A few specks or spots floating in the visual field of the eye are because of the

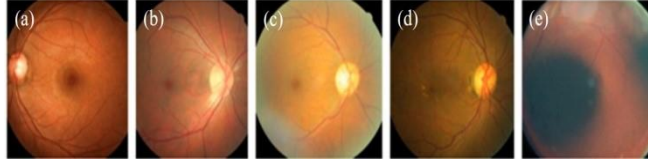


Fig. 1. Classification of DR: NPDR and PDR. NPDR is the early stage of DR, which comprises edema and hard exudates. Later stages comprise vascular occlusion, a restriction of blood supply to the retina, and an increase in macular edema, known as PDR. Images of retina with (a) No DR (b) Mild NPDR (c) Moderate NPDR (d) Severe NPDR (e) PDR

presence of DR. DR can be classified into two main stages as shown in Fig. 1, NPDR (Non-proliferative diabetic retinopathy) and PDR (Proliferative diabetic retinopathy). NPDR is the primary stage of diabetic eye disease. [5]. In NPDR, the tiny blood vessels leak and cause swelling of the retina [6]. People with NPDR have blurry vision. NPDR can be further classified as mild, moderate, and severe. PDR is the more advanced stage of diabetic eye disease [7]. In this stage, the retina starts growing new blood vessels called neovascularization [8]. These fragile new vessels often bleed into the vitreous. PDR is very serious as it causes loss of central and peripheral vision of a person.

The workflow diagram of the proposed system is shown in Fig. 2.

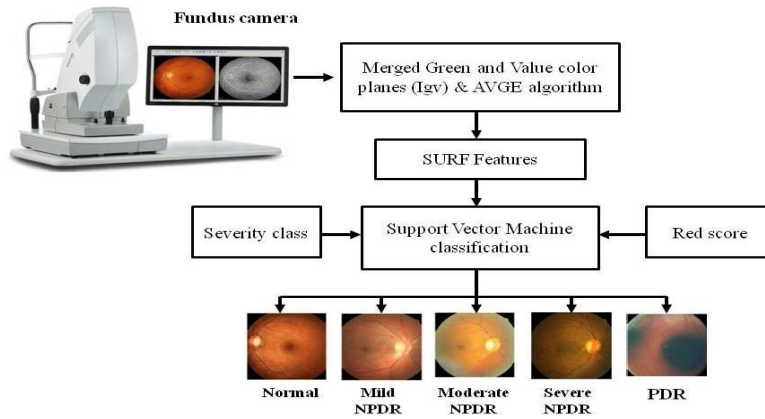


Fig. 2. Workflow diagram of the proposed system. The retinal fundus image is passed through the combined enhanced green and value color plane. The extracted SURF features, along with the red score and the DR severity level, are fed to the SVM classifier for predicting the level of severity.

The fundus camera captures the images of the retina. This image is pre-processed and the enhanced green and value color planes are extracted from it. The two-color planes

are combined and the AGVE algorithm is applied to it. Then the SURF algorithm is used to extract the strongest feature points. The red score feature is computed and normalized to a total number of pixels. DR severity level is obtained by calculating the ground truths of each of the abnormalities. Red score feature with the DR severity level is then added to the previous SURF feature vector to classify various stages of DR.

The remaining sections of the study are organized as follows. Section 2 presents the literature review. Section 3 presents the methodology of the proposed system. Results and discussions of the proposed work take place in Section 4 and 5 respectively. At last, Section 6 concludes the study.

2 Literature Review

Several automated algorithms have been over viewed by the authors for detecting and grading the severity of DR.

Pires and his group [9] introduced an effective method for directly assessing the refer-ability of patients without preliminary DR lesion detection. The accuracy of the proposed method was improved using SVM. Lachure and his team [10] developed an automatic screening of DR by detecting red and bright lesions using GLCM as a feature extraction technique in digital fundus images. The SVM outperformed better over KNN classifier in detecting the severity level of DR. Abbas et al. [11] developed a novel automatic recognition system for recognizing the five severity levels of diabetic retinopathy (SLDR) using visual features and a deep-learning neural network (DLNN) model.

A method for detecting DR was presented by Costa and his group [12] using a Bag-of-Visual Words (BoVW) method. Their work comprised extracting dense and sparse features using SURF and CNN from the image. The sparse feature SURF model outperformed well as compared with the dense feature CNN model. A fully automated algorithm using deep learning methods for DR detection was developed by Gargeya et al. [13]. Their work focused on preprocessing the fundus images and training the deep learning network with the data-driven features from the data set. The tree-based classification model classified the fundus image into grade 0 (no retinopathy) or grade 1 (severity from mild, moderate, severe, or proliferative DR). A hybrid machine learning system was proposed by Roy and his group [14] for DR severity prediction from retinal fundus images. Their work comprised CNNs with dictionary-based approaches trained for DR prediction. The resulting feature vectors were concatenated and a Random forest classifier was trained to predict DR severity.

Islam and his team [15] described an automated method using a bag of words model with SURF for DR detection in retinal fundus images. Their work comprised detecting the interesting SURF points, and the classification was performed using SVM. A computer-assisted diagnosis was introduced by Carrera and his team [16] to classify the

fundus image into one of the NPDR grades. The SVM and a decision tree classifier were used to figure out the retinopathy grade of each retinal image. Koh and his group [17] presented an automated retinal health screening system to differentiate normal image from abnormal (AMD, DR, and glaucoma) fundus images. They extracted the highly correlated features from the PHOG and SURF descriptors using the canonical correlation analysis approach. The system was evaluated using a tenfold cross-validation strategy using the k-nearest neighbor (k-NN) classifier.

A dictionary-based approach for severity detection of diabetic retinopathy was introduced by Leeza and her team [18]. Their work comprises creating the dictionary of visual features and detecting the points of interest using SURF algorithm. The images were further classified into five classes: normal, mild, moderate, and severe NPDR and PDR, using the radial basis kernel SVM and Neural Network. Gayathri and her team [19] have focused on the detection of diabetic retinopathy using binary and multiclass SVM. Their work comprised extracting Haralick and Anisotropic Dual Tree Complex Wavelet Transform (ADTCWT) features for reliable DR classification from retinal fundus images. Gadekallu et al. [20] developed a hybrid principal component analysis (PCA) firefly-based deep neural network model for the classification of diabetic retinopathy. Their work employed scalar technique for normalizing the dataset, PCA for feature selection, Firefly algorithm for dimensionality reduction, and machine learning classifiers and DNN for DR detection.

3 Methodology

The proposed method for estimating the severity levels of DR comprises diverse processes, such as preprocessing, segmentation, feature extraction, and classification. First, the original input image is transformed into a grayscale image. Then, the RGB and HSV color planes are extracted. The optic disk and the blood vessels are segmented. Further, the enhanced green and value sub color planes are merged and the AGVE algorithm is used to obtain the average grey value in a fundus image. The ground truth sum of each abnormality, such as microaneurysms, hemorrhages, hard exudates, and soft exudates, is used to calculate the severity level of a fundus image. The red score is generated and the SURF algorithm is used to extract the most important feature points from the fundus image. An SVM is trained for these features and the DR severity level is predicted. Fig. 3 shows the overall process of the proposed work.

The original image was converted to a grayscale image and the areas around the fundus image were masked using a threshold of 10 (equation 1 & 2).

$$g(x, y) = 0 \quad \forall f(x, y) < 10 \quad (1)$$

$$g(x, y) = f(x, y) \quad \forall f(x, y) \geq 10 \quad (2)$$

where $g(x, y)$ is the mask image and $f(x, y)$ is the gray scale image.

The original input color image is divided into three color planes R, G, and B. The green color plane is then selected and a maximum pixel intensity value was determined.

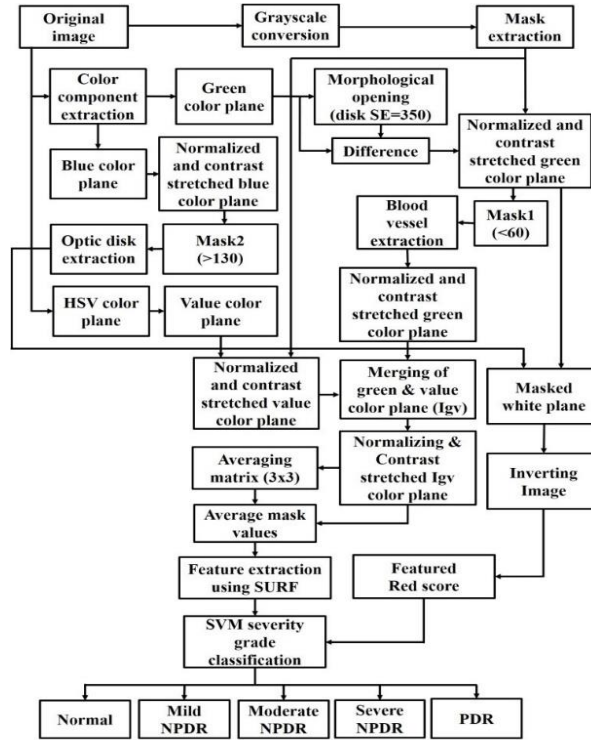


Fig. 3. The proposed method for predicting the severity levels of DR using the AGVE algorithm and SVM. An original input image is converted into a grayscale image. RGB and HSV color planes are extracted. The green and value sub color planes are merged and the AVGE algorithm is applied to extract the average gray value in the image. Then, the strongest feature points are extracted using the SURF algorithm. The SURF features, along with the red score feature and severity level, are used to train the SVM and the DR severity level is predicted.

A green channel enhancement was done in two steps. First, the masked pixels found from the masked image are set to 255 and second, the green channel color pixels are normalized (equation 3), and contrast stretch between 0 and 255.

$$h(x, y) = \frac{Ig(x, y) - \min(Ig(x, y))}{\max(Ig(x, y)) - \min(Ig(x, y))} \quad (3)$$

where, $I_g(x, y)$ is the green channel color image, $h(x, y)$ is the enhanced green channel color image, $\min(x, y)$ and $\max(x, y)$ are the minimum and maximum values of $I_g(x, y)$ and (x, y) is the current co-ordinates under consideration.

The blue color plane image was enhanced in the same way as that of the green color planes. The vessels visible in the green channel are enhanced by creating a mask with a threshold value of 60. The optic disk visible in the blue channel was masked with the thresholding level of 130. The original image was then converted into an HSV color plane and the value color plane and green color plane were merged with equal magnitude (equation 4).

$$I_{gv}(x, y) = 0.5 * I_g(x, y) + 0.5 * I_v(x, y) \quad (4)$$

where, I_g and I_v are the enhanced green color plane and value color planes.

The minima and the maxima of the newly obtained I_{gv} color plane are extracted and for masking purposes, all the max values are replaced by min values. I_{gv} image is then contrast stretched between 0 and 255. The average value from the entire I_{gv} fundus image is extracted using AGVE algorithm and all the masked pixels of the original I_{gv} are replaced by the average value calculated. This image is called I_{AGVE} image.

3.1 The Average Gray Value Extraction (AGVE) algorithm

The AGVE is a novel technique to extract the average grey level value of a fundus image. Fig. 4 depicts an illustration of the AGVE algorithm.

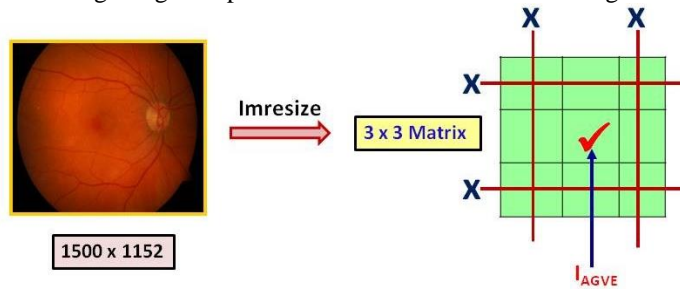


Fig. 4. Illustration of the AGVE algorithm.

Algorithm:

Step1. The I_{gv} image is transformed into a matrix of 3x3, given that the fundus image comprises a round border.

Step2. All the rows and columns that correspond to an edge are ignored for the averaging purpose.

Step3. Select the central pixel to ensure the maximum accuracy with the grey scale value extraction.

The image was then given to the mapping function that saturates top 1 % and bottom 1 % of all the pixel values to remove any spike noise to get the maximum information. This saturated image was then sent to the SURF algorithm for feature extraction and the strongest 320 feature points were considered as feature matrix. The DR severity grading was performed by calculating the ground truths of each of the abnormalities and generating red score for each image.

3.2 Red Score Calculation

The green channel image extracted from the original image was morphologically opened with a structural element (disk) of a size of 350 pixels to form the complete background picture. It was then subtracted from the green channel image to enhance the blood vessels and reddish parts in the eye. The outside image was then masked with white value and all the values below 50 are preserved while the remaining values are converted as 255. This image was then normalized (equation 3 & 4) and scaled up to 0 and 255. The image negative was then computed at a grayscale level. Finally, the red score feature was computed and normalized to a total number of pixels. This red feature score was then added to the previous 320 feature vector for severity classification.

3.3 Severity Level Generation

To gain the supervisory severity level the ground truths of four types of abnormalities such as hard exudates, soft exudates, microaneurysms, and hemorrhages from the DIARETDB1 dataset were used. All the four types of output images were binarized using Otsu's method and their corresponding sum was calculated. The binarized ground truth image of hemorrhage was used and all the four connected component objects were then separated and the total number of objects was computed for that image.

The severity level was then defined depending upon the abnormality and count in the images.

Level 1: Ground truth score of all abnormalities is Zero. Indicates no DR and the person is normal.

Level 2: Ground truth score of the microaneurysms is greater than zero and all other scores are zero. Indicates mild NPDR.

Level 3: Ground truth score of the hemorrhages or microaneurysms greater than zero then the flag is set and the exudates score is checked to be positive. Indicates moderate NPDR.

Level 4: Hemorrhage count greater than 20. Indicates severe NPDR.

Level 5: None of the severity maps matched. Indicates PDR.

Finally, the extracted SURF features, red score count and severity class were fed to the SVM classifier and the severity classification model was trained and tested.

4 Results

DIARETDB1 dataset was used for the experimentation purposes. Images were captured with the 50-degree field-of-view digital fundus camera with varying imaging settings controlled by the system and the experimentation was performed in MATLAB 2019a. The dataset comprises ground truths of four types of abnormalities, such as hard exudates, soft exudates, microaneurysms, and hemorrhages.

The performance of the proposed system has been validated using 76 images from the dataset. Out of which randomize 70% images were used for training and the remaining 30% were reserved for testing. This process was sequentially repeated 5 times to optimize the final SVM model. The outputs of all the 76 images were classified into 5 different severity levels. It was seen that only first 4 levels were assigned to the fundus images while the last level was ignored throughout the calculations. As it was assumed that the occurrence frequency of this level is very less in the DIARETDB1 dataset.

The 8% randomly selected images were then tested, and the accuracy was computed. To compute accuracy, the number of correctly classified DR images was divided by the total number of DR images in the dataset. Hence, if the model classified 8 DR images accurately out of 10, then the accuracy of the model would be 80%.

Result analysis

Fig. 5 visualizes the output of the proposed system at various phases of DR severity level detection.

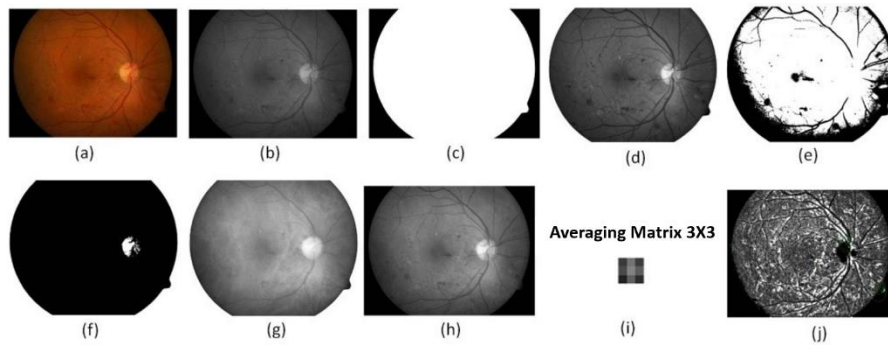


Fig. 5. Output at various stages for the proposed method during DR severity detection. (a) Original image of the retina. (b) Grayscale image. (c) Mask image. (d) Enhanced green color plane. (e) Extracted blood vessels. (f) Optic disc extraction. (g) Enhanced value color plane. (h) Enhanced combined green & value color planes. (i) Averaging matrix 3X3. (j) SURF feature points.

The confusion matrix of the proposed system is shown in Table 1. Out of total 76 images, only 1 image was found to be inaccurately classified. The Level 2 image was categorized as Level 3 image. There were no images of severity level 5 hence, they are not shown in the confusion matrix.

Table 1. Confusion matrix
Actual

Predicted	Severity Level	Level 1	Level 2	Level 3	Level 4	Image Count
	Level 1	5	0	0	0	5
Level 2	0	18	0	0	18	
Level 3	0	1	40	0	41	
Level 4	0	0	0	12	12	
Image Count	5	19	40	12	76	

Table 2 and Fig.6. shows a detailed classifier outcome of the proposed model in terms of four accuracy measures.

Table 2. Performance measures of DR severity levels

Severity Level	Accuracy (%)	Specificity (%)	Sensitivity (%)	F1 score
Level 1	100	100	100	1
Level 2	98.68	100	95	0.97
Level 3	98.68	98	100	0.99
Level 4	100	100	100	1

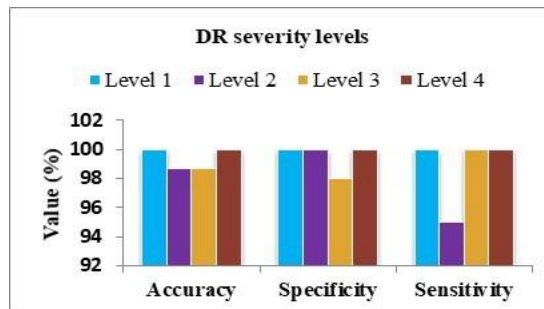


Fig. 6. Comparison of DR severity levels based on performance metrics

It is observed that the DR images under level 1 (normal) category are classified by the accuracy of 100%, sensitivity of 100%, specificity of 100%, and F1 score of 1. Next, the DR images under level 2 categories are classified by the accuracy of 98.68%, sensitivity of 95%, specificity of 100%, and F1 score of 0.97. Similarly, the DR images under level 3 categories are classified by the accuracy of 98.68%, sensitivity of 100%, specificity of 98%, and F1 score of 0.99. In the same way, the DR images under level 4 are classified by the accuracy of 100%, sensitivity of 100%, specificity of 100%, and F1 score of 1. These values shows that the proposed system effectively grades the DR images under respective classes.

The accuracy obtained for the different number of folds in five test runs of the proposed system is shown in Table 3. During the 5 different runs, the average accuracy gradually increases from 54.64% to 98.68%. The standard deviation at the lowest accuracy was around 0.89 and at 5-fold validation it could reach up to 0.45. The deviation for the intermediate runs was found to be 1.51. For single fold cross-validation, the average accuracy obtained was 54.64%, which was the lowest among all the folds tested. The average accuracy increases with an increasing number of folds, with the highest average accuracy of 98.68% being obtained at five-fold cross-validation. Throughout the five test runs the accuracy values obtained are fairly consistent for each number of folds. Overall, the trend of accuracy was seen improving till five fold validation and then got saturated. Hence, we decided to select five folds as the optimal number of folds.

Table 3. Accuracy values for varying number of folds for five test runs

Number of Folds	Accuracy (%)						Standard Deviation
	1st Run	2nd Run	3rd Run	4th Run	5th Run	Average	
1	54.5	52.6	54.5	56.4	55.2	54.64	0.89
2	73.3	72.1	72.4	74.2	73.3	73.06	0.51
3	94.9	93.2	91.2	92.8	95.4	93.5	1.51
4	96.7	95.5	94.5	96.5	97.4	96.12	0.9
5	99.3	98.2	98.6	97.4	100	98.7	0.45

5 Discussions

The comparison of the proposed method with the existing methods in the literature is shown in Table 4. Out of all the systems reported in the literature, our system could achieve one of the highest accuracy of 98.68% and sensitivity of 98.75%. Similarly, the proposed method could deliver the highest specificity of 99.5% which was similar to as reported by Lachure et al. [10]. The Area Under Curve (AUC) was not computed by

Table 4. Performance comparison of other algorithms for DR detection

Author	Technique	Accuracy (%)	Sensitivity (%)	Specificity (%)	Area Under Curve (AUC)
Pires et al. [9]	Extraction of mid level features- BossaNova and Fisher Vector and Fisher Vector	--	--	96.4	--
Lachure et al. [10]	Morphological operations for detecting red and bright lesions and GLCM	--	90	100	--
Abbas et al. [11]	Visual features and a deep-learning neural network (DLNN) model	--	92.18	94.5	0.924
Costa et al. [12]	Dense and sparse feature extraction using CNN and SURF	--	--	--	0.93
Gargeya et al. [13]	Deep learning network with data driven features	--	94	98	0.97
Roy et al. [14]	CNNs with generative and discriminative bag-of-word dictionary	61	92	--	--
Islam et al. [15]	SURF features with Kmeans clustering	94.4	94	94	0.95
Carerra et al. [16]	Quantitative feature extraction	85	94.6	--	--
Koh et al. [17]	PHOG and SURF descriptors using the canonical correlation analysis approach	96.21	95	97.42	--
Leeza et al. [18]	Computation of descriptive features through SURF and histogram of oriented gradients	98.3	95.92	98.9	--
Gayathri et al. [19]	Haralick and Anisotropic Dual-Tree Complex Wavelet Transform (ADTCWT) features	97.42	97.5	0.994	--
Gadekallu et al. [20]	Principal Component Analysis (PCA) and firefly based deep neural network model	73.8	83.6	83.6	--
Alyoubi [21]	Deep learning based models for DR detection and localization of DR lesions	89	97.3	89	--
Proposed method	Severity classification using SURF features from the enhanced green and value plane and AGVE algorithm	98.68	98.75	99.5	1

most of the reported literature, but amongst the papers that reported it, the proposed method had the maximum AUC of 1. The average F1 score for all the severity levels was found out to be 0.99. The proposed method uses a unique combination of the green sub-color plane from RGB and the value sub-color plane from the HSV plane to enhance the overall features of the fundus image. An AGVE algorithm was applied on the merged plane to extract the important information from the eye. The red score generated enabled to highlight the reddishness of the eye. Due to the unique combination of the color planes and the selection of vital features using AGVE and SURF, the proposed method was able to accurately detect the severity grade level of DR from a fundus image. Hence, our method could achieve the highest accuracy among the other methods reported literature.

6 Conclusion

Diabetic retinopathy (DR) is a vision-related consequence of long-term diabetes. If not treated on time can lead to complete loss of vision. As a result, an early diagnosis and a concise approach for identifying and rating the severity level of DR is required. Thus, our suggested study comprises four levels of severity classification approach employing an SVM classifier that predicts different levels of DR severity. The system performed pre-processing on the input fundus images to extract the enhanced green and value plane, which were then merged. The AGVE algorithm was used to highlight important details in the merged green and value plane image. Finally, the SURF and our novel red score method were used to extract the features of the fundus images, which were further used to train an SVM classifier. The unique method of feature extraction enabled the classifier to detect the severity accurately in the fundus images. Our system achieved an average accuracy of 98.68% and an average F1 score of 0.99. The proposed system can be easily deployed on the currently available equipment at hospitals and laboratories, which would enable the doctors to detect DR accurately and efficiently.

References

1. M. M. Nentwich and M. W. Ulbig, "Diabetic retinopathy-ocular complications of diabetes mellitus," *World journal of diabetes*, vol. 6, no. 3, p. 489, 2015.
2. S. B. Junior and D. Welfer, "Automatic detection of microaneurysms and hemorrhages in color eye fundus images," *International Journal of Computer Science & Information Technology*, vol. 5, no. 5, p. 21, 2013.
3. M. Fruttiger, "Development of the retinal vasculature," *Angiogenesis*, vol. 10, no. 2, pp. 77–88, 2007.
4. M. S. Dwyer, L. J. Melton, D. J. Ballard, P. J. Palumbo, J. C. Trautmann, and C.-P. Chu, "Incidence of diabetic retinopathy and blindness: a population-based study in rochester, minnesota," *Diabetes Care*, vol. 8, no. 4, pp. 316–322, 1985.

5. M. Mesquida, F. Drawnel, and S. Fauser, "The role of inflammation in diabetic eye disease," in *Seminars in immunopathology*, vol. 41, no. 4, Springer, 2019, pp. 427–445.
6. R. S. Maher, S. N. Kayte, S. T. Meldhe, and M. Dhopeswarkar, "Automated diagnosis non-proliferative diabetic retinopathy in fundus images using support vector machine," *International Journal of Computer Applications*, vol. 125, no. 15, 2015.
7. J. A. Davidson, T. A. Ciulla, J. B. McGill, K. A. Kles, and P. W. Anderson, "How the diabetic eye loses vision," *Endocrine*, vol. 32, no. 1, pp. 107–116, 2007.
8. J.-H. Chang, E. E. Gabison, T. Kato, and D. T. Azar, "Corneal neovascularization," *Current opinion in ophthalmology*, vol. 12, no. 4, pp. 242–249, 2001.
9. R. Pires, S. Avila, H. F. Jelinek, J. Wainer, E. Valle, and A. Rocha, "Beyond lesion-based diabetic retinopathy: a direct approach for referral," *IEEE journal of biomedical and health informatics*, vol. 21, no. 1, pp. 193–200, 2015.
10. J. Lachure, A. Deorankar, S. Lachure, S. Gupta, and R. Jadhav, "Diabetic retinopathy using morphological operations and machine learning," in *2015 IEEE international advance computing conference (IACC)*. IEEE, 2015, pp. 617–622.
11. Q. Abbas, I. Fondon, A. Sarmiento, S. Jimenez, and P. Alemany, "Automatic recognition of severity level for diagnosis of diabetic retinopathy using deep visual features," *Medical & biological engineering & computing*, vol. 55, no. 11, pp. 1959–1974, 2017.
12. P. Costa and A. Campilho, "Convolutional bag of words for diabetic retinopathy detection from eye fundus images," *IPSN Transactions on Computer Vision and Applications*, vol. 9, no. 1, pp. 1–6, 2017.
13. R. Gargeya and T. Leng, "Automated identification of diabetic retinopathy using deep learning," *Ophthalmology*, vol. 124, no. 7, pp. 962–969, 2017.
14. P. Roy, R. Tennakoon, K. Cao, S. Sedai, D. Mahapatra, S. Maetschke, and R. Garnavi, "A novel hybrid approach for severity assessment of diabetic retinopathy in colour fundus images," in *2017 IEEE 14th International Symposium on Biomedical Imaging (ISBI 2017)*. IEEE, 2017, pp. 1078–1082.
15. M. Islam, A. V. Dinh, and K. A. Wahid, "Automated diabetic retinopathy detection using bag of words approach," *Journal of Biomedical Science and Engineering*, vol. 10, no. 5, pp. 86–96, 2017.
16. E. V. Carrera, A. Gonzalez, and R. Carrera, "Automated detection of diabetic retinopathy using svm," in *2017 IEEE XXIV international conference on electronics, electrical engineering and computing (INTERCON)*. IEEE, 2017, pp. 1–4.
17. J. E. Koh, E. Y. Ng, S. V. Bhandary, A. Laude, and U. R. Acharya, "Automated detection of retinal health using phog and surf features extracted from fundus images," *Applied Intelligence*, vol. 48, no. 5, pp. 1379–1393, 2018.
18. M. Leeza and H. Farooq, "Detection of severity level of diabetic retinopathy using bag of features model," *IET Computer Vision*, vol. 13, no. 5, pp. 523–530, 2019.
19. S. Gayathri, A. K. Krishna, V. P. Gopi, and P. Palanisamy, "Automated binary and multiclass classification of diabetic retinopathy using haralick and multiresolution features," *IEEE Access*, vol. 8, pp. 57 497–57 504, 2020.
20. T. R. Gadekallu, N. Khare, S. Bhattacharya, S. Singh, P. K. Reddy Maddikunta, I.-H. Ra, and M. Alazab, "Early detection of diabetic retinopathy using pca-firefly based deep learning model," *Electronics*, vol. 9, no. 2, p. 274, 2020.